

- 11 Heijnen, J. J., Roels, J. A., and Stouthamer, A. H., Application of balancing methods in modelling the penicillin fermentation. *Biotechnol. Bioeng.* 21 (1979) 2175–2201.
- 12 Hu, W.-S., and Demain, A. L., Regulation of antibiotic biosynthesis by utilizable carbon sources. *Proc. Biochem.* 14 (1979) 2–6.
- 13 Jantsch, E., *The Self-organization of the Universe*. Pergamon Press, Oxford 1980.
- 14 Meyer, H. P., Reference fermentations, in: *Physical Aspects of Bioreactor Performance*. Chapt. 9. Ed. W. Crueger et al., Dechema 1987.
- 15 Moser, A., Multi-purpose bioreactor for process kinetic analysis. *Advances in fermentation*. Suppl. *Proc. Biochem.* (1983) 202–211.
- 16 Moser, A., Bioprocess kinetics: Interactions between biology and physics, in: *Proc. 8th Intern. Biotechnol. Symp.*, Paris 1988. Soc. Franç. Microbiol., vol. 1, 386–397.
- 17 Moser, A., Model bioreactors: a powerful contribution to biotechnical methodology. *Trends Biotechnol.* 7 (1989) in press.
- 18 Moser, A., Bioreactors and their use for the optimisation of process parameters, in: *Proc. 1st Eur. Congr. Biotechnol.*, Interlaken 1978, vol. 1, 88–91.
- 19 Moser, A., *Bioprocess technology-kinetics and reactors*. Springer Inc., New York 1988.
- 20 Moser, A., Formal macro-approach to bioprocessing-models with analogies. *Acta biotechnol.* 3 (1983) 195–216.
- 21 Moser, A., and Schneider, H., Modelling secondary metabolites: case pleuromulin, in: *Proc. 4th Int. Conf. Computer Appl. in Ferm. Technol.*, 93–104. Eds N. M. Fish. Elsevier Appl. Science, London 1989.
- 22 Mou, D. G., and Cooney, C., Application of dynamic calorimetry for monitoring fermentation processes. *Biotechnol. Bioeng.* 18 (1976) 1371–1392.
- 23 Park, Y., Davis, M., and Willis, D., Analysis of a continuous, aerobic, fixed-film bioreactor. I. Steady state behavior. *Biotechnol. Bioeng.* 26 (1984) 457–467.
- 24 Peringer, P., Blanchère, H., Corrieu, G., and Lane, A. G., Mathematical model of the kinetics of growth of *Saccharomyces cerevisiae*. *Biotechnol. Bioeng. Symp.* 4 (1973) 27–42.
- 25 Pirt, S. J., The Penicillin Fermentation. *Kem. Ind.* 34 (1985) 13–19.
- 26 Reuss, M., Modelling and optimization of processes, in: *Proc. 8th Int. Biotechnol. Symp.*, Paris 1988. Soc. Franç. Microbiol., vol. 1, 523–536.
- 27 Roels, J. A., Application of macroscopic principles to microbial metabolism. *Biotechnol. Bioeng.* 22 (1980) 2457–2514.
- 28 Sonnleitner, B., and Käppeli, O., Growth of *Saccharomyces cerevisiae* is controlled by its limited respiratory capacity: Formulation and verification of a hypothesis. *Biotechnol. Bioeng.* 28 (1986) 927–937.
- 29 Stephanopoulos, G., and San, K. Y., Studies on on-line bioreactor identification. I. Theory. *Biotechnol. Bioeng.* 26 (1984) 1176–1188.
- 30 Strässle, C., Sonnleitner, B., and Fiechter, A., A predictive model for the spontaneous synchronisation of *Saccharomyces cerevisiae* grown in continuous culture. II. Experimental verification. *J. Biotechnol.* 9 (1989) 191–208.
- 31 Sweere, A., Mesters, J., Luyben, K., and Kossen, N., Regime analysis of the baker's yeast production, in: *Proc. Int. Conf. Bioreactor Fluid Dynamics*. BHRA Press, Cambridge 1986, 217–230.
- 32 Sweere, A., Van Dalen, J., Kishori, E., Luyben, K., and Kossen, N., Theoretical analysis of the baker's yeast production: An experimental verification at the laboratory scale. Part 2: Fed-batch fermentations. *Bioprocess Engng* 4 (1989) 11–18.
- 33 Varela, F., Maturana, H. R., and Uribe, R., Autopoiesis. The organization of living systems, its characterization and a model. *Biosystems* 5 (1974) 187–196.
- 34 Williams, F. M., A model of cell growth dynamics. *J. theor. Biol.* 15 (1967) 190–207.
- 35 Wöhrer, W., and Röhr, M., Regulatory aspects of baker's yeast metabolism in aerobic fed-batch cultures. *Biotechnol. Bioeng.* 23 (1981) 567–581.

0014-4754/89/11-12/1035-07\$1.50 + 0.20/0

© Birkhäuser Verlag Basel, 1989

## Determination of oxygen gradients in single Ca-alginate beads by means of oxygen-microelectrodes

J. Beunink<sup>a</sup>, H. Baumgärtel<sup>b</sup>, W. Zimelka<sup>b</sup> and H.-J. Rehm<sup>\*a</sup>

<sup>a</sup> *Institut für Mikrobiologie, Universität Münster, Corrensstr. 3, D-4400 Münster (Federal Republic of Germany), and*

<sup>b</sup> *Max-Planck-Institut für Systemphysiologie, Rheinlanddamm 201, D-4600 Dortmund (Federal Republic of Germany)*

**Summary.** Oxygen concentrations were measured in single Ca-alginate beads using polarographic microneedle electrodes. To obtain reliable results the effects of mechanical pressure on the electrode as well as the influence of free  $\text{Ca}^{2+}$ -ions had to be compensated. No oxygen gradients were detectable in cell-free alginate beads, whereas in beads with entrapped cells of *Enterobacter cloacae* steep oxygen gradients were observed. The steepness of these gradients depended on the bacterial growth in the gel. At the end of the logarithmic phase of growth the maximum depth of oxygen penetration into a bead of about 3 mm in diameter was in the range of 150  $\mu\text{m}$ ; i.e. nearly 70 % of the volume of the alginate beads was free of oxygen.

**Key words.** Oxygen gradients; Ca-alginate;  $\text{pO}_2$ -microelectrodes; immobilized microorganisms.

### Introduction

Entrapment in alginate gels is a technique often used for the immobilization of microbial cells. One disadvantage of the method is the restriction of substrate transport inside the particles to diffusion. This is especially important for oxygen, the maximum concentration of which in air-saturated media is only about 230  $\mu\text{mol/l}$  (at 30 °C), so that in central parts of the immobilisates oxygen-limiting conditions may appear<sup>12</sup>.

On the basis of experimental results concerning the oxygen uptake rate of immobilized cells<sup>13</sup>, the maximum penetration depth of oxygen in alginate immobilisates was calculated to be 50–200  $\mu\text{m}$ <sup>6</sup>, whereas the critical particle diameter for a sufficient oxygen supply, depending on the cell concentration and respiration rate, could be calculated to be less than 1 mm<sup>9</sup>.

According to these findings, the greater part of the alginate beads, the diameters of which are usually in the range of 2–5 mm, should be oxygen-free. Organisms in

the central parts of the beads may therefore live under anaerobic conditions.

This assumption is confirmed by results for the activity of immobilized methanogenic bacteria in the presence of oxygen<sup>17</sup> and the increased rate of nitrogen fixation by immobilized cells of *Azotobacter chroococcum*<sup>18</sup>. Other examples are the synchronous nitrification and denitrification by coimmobilisates of *Nitrosomonas europaea* and *Paracoccus denitrificans*<sup>19</sup> and our own results concerning synchronous reductive and oxidative reactions during the microbial degradation of DDT by coimmobilisates of *Enterobacter cloacae* and *Alcaligenes* sp.<sup>4</sup>.

Direct measurements of molecular oxygen within microbial aggregates have been performed only for bacterial slimes and films<sup>5,7</sup> and for mycelial pellets<sup>15,25</sup>. Until now no such measurements have been carried out in single calcium-alginate beads, although this is the only direct method for the examination of aerobic and anaerobic parts within the immobilisates. In this investigation we describe the use of the oxygen microelectrode according to Baumgärtl and Lübberts<sup>2</sup> for the direct measurement of oxygen gradients within single alginate beads with entrapped cells of a strain of *Enterobacter cloacae* which we used in a previous study<sup>3</sup>.

### Materials and methods

#### Microorganism and growth conditions

The experiments were carried out with cells of a strain of *Enterobacter cloacae* which has already been used for DDT-degradation studies<sup>4</sup>.

Cells were grown in a mineral salts medium of the following composition:  $\text{KH}_2\text{PO}_4$ : 1.90 g/l;  $\text{Na}_2\text{HPO}_4$ : 0.88 g/l;  $(\text{NH}_4)_2\text{SO}_4$ : 1.32 g/l,  $\text{MgSO}_4 \times 7 \text{H}_2\text{O}$ : 0.2 g/l;  $\text{Ca}(\text{NO}_3)_2$ : 0.5 mg/l;  $\text{FeSO}_4$ : 0.5 mg/l; trace element solution<sup>22</sup>: 1.0 ml/l; yeast extract: 0.1 g/l; glucose: 5.0 g/l (pH 6.7).

Free cells were cultivated in 300-ml Erlenmeyer flasks with baffles, on a reciprocal shaker with 150 rpm. Ca-alginate entrapped cells were cultivated in a 300-ml airlift reactor. In all experiments the medium/alginate ratio was 2:1. The aeration rate was 1.7 vvm. The reactor design permitted the removal of single alginate beads under sterile conditions during the fermentation. All experiments were carried out at 30 °C.

#### Immobilization

Microorganisms were immobilized by entrapment in 3% Ca-alginate as described previously<sup>10</sup>. The initial cell concentration was  $2 \times 10^8$  cells per ml Na-alginate. The diameter of the Ca-alginate beads was in the range of 3 mm as determined with a microscope. Na-alginate (Manugel-DJX) was obtained from Kelco/AIL (Hamburg).

#### Determination of microbial growth

Growth of *Enterobacter cloacae* inside the Ca-alginate was determined by dissolving alginate beads in 50 mM

sodium-hexametaphosphate and counting suitably diluted samples in a Thoma chamber.

#### Determination of calcium-release by Ca-alginate

A defined quantity of Ca-alginate beads was suspended in 10 ml of double-distilled water for 1 h. Calcium ions in the supernatant were determined by atomic absorption spectrometry using a Pye/Unicam SP9 atomic absorption spectrometer. The wavelength used was 422.7 nm.

#### Oxygen-microelectrodes

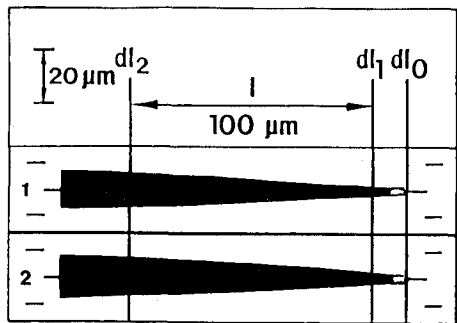
Oxygen was measured polarographically with a membrane-covered microcoaxial needle electrode. This electrode is made of a Pt-cathode fused in glass and a thin layer of Ag/AgCl as a reference electrode, both situated behind the same membrane. This membrane was made from thin films of collodion and polystyrene. Only electrodes with a recess were used, because this type shows low 'stirring effects' (mean value of 20 electrodes = 1.7%) and good membranization properties. Response time,  $t_{90}$ , of the electrodes was 50–300 ms, depending on recess length and membrane thickness. The response time of the measuring system as a whole was 0.4–1.0 s. The oxygen sensitivity of the electrodes was about 0.8 pA/Torr. The stability of the oxygen reduction current in air-saturated Theorell buffer solution and at an optimal polarization voltage was in the range of 0.5–1.5%/h (25 °C). Other typical technical data for the microelectrodes used are summarized in the table shown in figure 1. Details of construction and manufacturing of these oxygen microelectrodes have been published elsewhere<sup>2</sup>.

#### Oxygen concentration measurements

Oxygen concentration measurements in single Ca-alginate beads were carried out in a simple airlift loop reactor<sup>25</sup>. All measurements were carried out exclusively with an aeration rate of 1.7 vvm. The fermentation medium without N-sources was used as measuring medium to prevent further propagation of the cells. For complex-binding of free  $\text{Ca}^{2+}$ -ions, which may be released from the calcium-alginate, 0.5 mM bis(aminoethyl)-glycol-ether-N,N,N',N'-tetraacetic acid  $\times 4 \text{Na}^+$  ( $\text{Na}_4$  EGTA) were added.

The alginate bead to be measured was fixed with a wire loop in the airlift reactor. By use of a micromanipulator (Zeiss, Oberkochen) the microelectrode was brought towards the bead. Puncture of the bead in a radial direction was performed by electrode movements in steps of 25  $\mu\text{m}$ . The electrode-signal was measured with a nanoAmpèremeter (Knick, Berlin) and registered continuously. The polarization voltage (700 mV) was supplied by a highly stabilized voltage supply (MPI, Dortmund).

Before each measurement, calibration of the electrodes was carried out in the measuring medium as well as in the alginate beads with oxygen-free nitrogen, air and a 1:1-



#	$\frac{dl_1(\mu m)}{dl_2(\mu m)}$	$\star \tan \alpha$	$\frac{R_1(\mu m)}{Pt \varnothing (\mu m)}$	$\frac{R_1}{d}$	$\frac{I_{air}(nA)}{I_{N_2}(nA)}$	$\frac{I_{air}}{I_{N_2}}$	$R_c(\%)$
1	$\frac{4.2}{14.0}$	2.8	$\frac{5.8}{2.9}$	2.0	$\frac{0.120}{0.003}$	40	0.9
2	$\frac{4.2}{14.0}$	2.8	$\frac{5.0}{2.9}$	1.7	$\frac{0.115}{0.001}$	115	2.6

$dl_1$  electrode diameter at 14  $\mu m$  from the electrode tip  $dl_0$   
 $dl_2$  electrode diameter at 114  $\mu m$  from the electrode tip  $dl_0$   
 $\tan \alpha = \frac{r_2 - r_1}{100}$   
 $r_1, r_2$  electrode radius [ $\mu m$ ] at  $dl_1$  and  $dl_2$  respectively  
 $R_1$  length of the recess  
 $Pt \varnothing$  diameter of the Pt-cathode at the electrode tip  
 $I_{air}$  signal in air saturated medium  
 $I_{N_2}$  signal in nitrogen saturated medium  
 $Re$  'stirring effect'

The dimensions refer to non-membranized electrodes as determined with a light microscope.

Figure 1. Typical technical data for the  $pO_2$ -microelectrodes used in this investigation.

mixture of air and pure nitrogen obtained by using a gas mixing pump (Wösthoff, Bochum). Since the amount of oxygen which is reduced at the Pt-surface is proportional to the oxygen pressure on the outside of the membrane, the electrodes measure the oxygen activity or the equivalent partial pressure of dissolved oxygen of the media. The oxygen concentration is formed according to Henry's law:

$$C_0 = \alpha \cdot pO_2$$

where  $C_0 = O_2$  concentration in  $cm^3/cm^3$   
 $\alpha$  = solubility coefficient in  $cm^3/(cm^3 \cdot Torr \text{ or } kPa)$ , and  
 $pO_2 = O_2$  partial pressure in Torr or kPa

The molar concentrations is given by the equation

$$C \text{ (in mol/cm}^3\text{)} = \frac{pO_2}{H}$$

$$\text{with the Henry constant } H = \frac{22400 \cdot (760)}{\alpha}$$

## Results

### Oxygen profiles in Ca-alginate

The measurement of oxygen profiles in single Ca-alginate beads by means of microelectrodes was affected by two main methodological difficulties; the effect of mechanical pressure during the penetration of the needle-electrode and the disturbance of the electrode function by free  $Ca^{2+}$ -ions.

The steep decreases of the electrode signal with every step inside alginate beads (fig. 2) resulted from a mechanical pressure of the gel on the microelectrode. By use of a stepwise puncture-technique with periodical withdrawals of the electrode this effect was compensated. In our case we used a 50- $\mu m$  step-in immediately followed by a 25- $\mu m$  step-out. Using this technique, uniform electrode signals were obtained (fig. 2).

As can also be seen from figure 2 a constant reduction of the electrode signal appeared as the alginate surface was reached by the tip of the electrode. This signal reduction was in the range of 9–13% of the signal in air-saturated medium and varied with the electrode used. This effect has been used for the exact determination of the bead surface.

Free  $Ca^{2+}$ -ions had a severe effect on the function of the oxygen-microelectrodes used in our investigation. Irregular discharging and a strong drifting of the signal to the point of complete lack of sensitivity to oxygen were the typical effects (fig. 3 A). This is especially important for microelectrode measurements in Ca-alginate which may release C-ions in consequence of insufficient washing during the making of the beads. By optimization of the washing processes the concentration of free  $Ca^{2+}$ -ions could be drastically lowered. Figure 4 gives the results for the calcium-release of Ca-alginate beads in relation to the method of washing. Washing twice with 1 l of 0.9% NaCl (per 100 ml alginate) for 20 min, followed by a single wash with 1 l of 0.9% NaCl + 0.5 mM  $Na_4EGTA$  (per 100 ml alginate) for 20 min was the best method for elim-

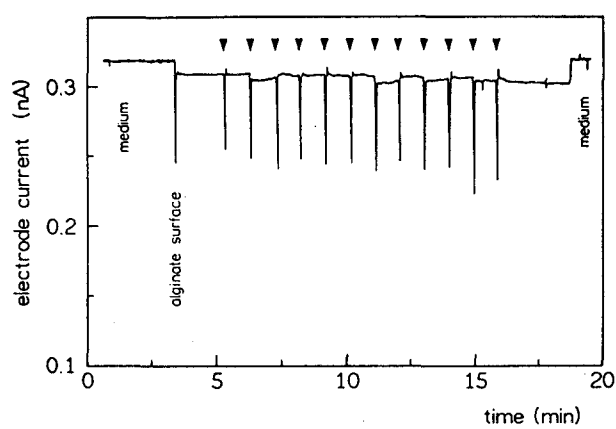


Figure 2. Section through an alginate bead showing the pressure effect and its compensation by a puncture technique with stepwise removal of the electrode. Arrows indicate 50- $\mu m$  steps-in immediately followed by 25- $\mu m$  steps-out (original record).

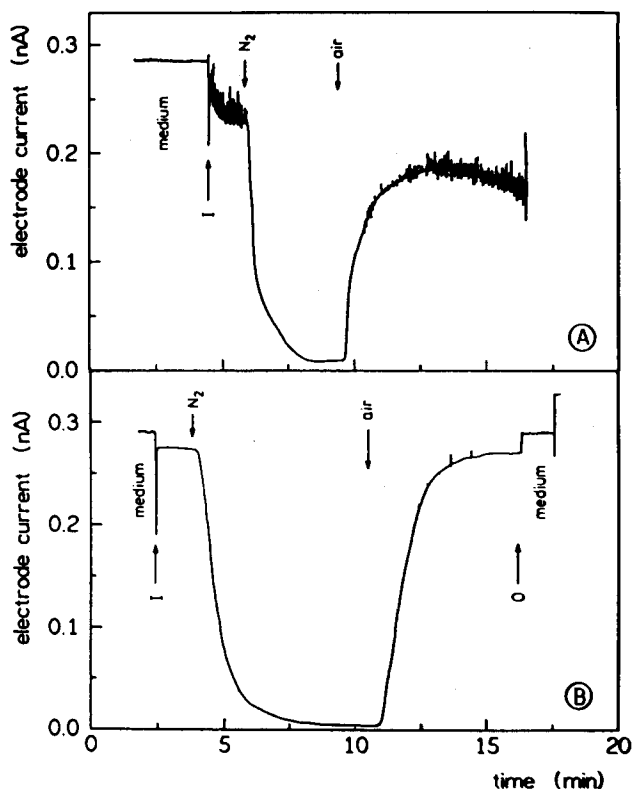


Figure 3. Effects of free Ca-ions on microelectrode function in Ca-alginate: irregular discharging and strong drifting of the electrode signal (A), and its elimination by optimized washing of the beads and addition of 0.5 mM  $\text{Na}_4\text{EGTA}$  (B) (original records). I, electrode inside the bead; O, electrode outside the bead.

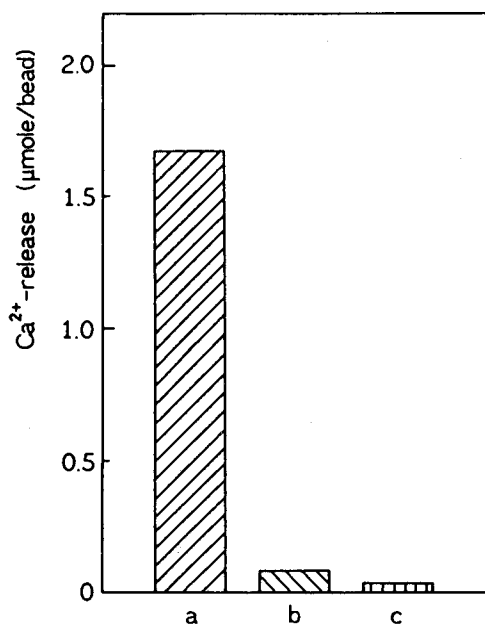


Figure 4. Release of calcium ions by Ca-alginate beads, showing dependence on the washing procedures during the making of the beads.

- Washing with 1.5 l 0.9% NaCl on a filter nozzle.
- Twice washing with 1.0 l 0.9% NaCl for 20 min.
- Twice washing with 1.0 l 0.9% NaCl for 20 min followed by a single washing with 1.0 l 0.9% NaCl + 0.5 mM  $\text{Na}_4\text{EGTA}$  for 20 min.

inating non-alginate bound Ca-ions. Alginate-bound Ca-ions as well as EGTA-bound ions had no disturbing effects on the electrode function (fig. 3 B). The stability of the Ca-alginate beads was not affected by the addition of  $\text{Na}_4\text{EGTA}$ .

#### Diffusion layer around Ca-alginate beads

All measurements in single alginate beads were carried out in flowing media (gasing rate 1.7 vvm), allowing convective oxygen transfer from the bulk-phase towards the alginate beads. Despite the bulk flow a diffusion layer around the alginate particles may be formed in which the oxygen concentration differs from that in the bulk-phase. To investigate whether such a diffusion layer was present, oxygen profile measurements from the bulk-phase to the alginate surface were carried out with cell-free and with cell-loaded alginate beads.

In the presence of bulk convective flow no oxygen diffusion layer could be detected around either the cell-free or the cell-loaded alginate beads within the local resolution of 25  $\mu\text{m}$ . In every case the oxygen concentration near the alginate surface equaled that in the stirred bulk-phase.

#### Oxygen gradients in cell-free and cell-loaded alginate beads

No oxygen gradient could be detected in cell-free alginate beads. The oxygen concentration inside the beads equaled that of the bulk-medium, except for the small  $\text{O}_2$ -change which demonstrates the altered diffusion conditions between medium and alginate bead. In contrast to this finding, beads loaded with growing cells of *E. cloacae* showed a sharp decrease in oxygen concentration a few micrometers below the alginate surface (fig. 5). About 150  $\mu\text{m}$  below the surface no oxygen was detectable.

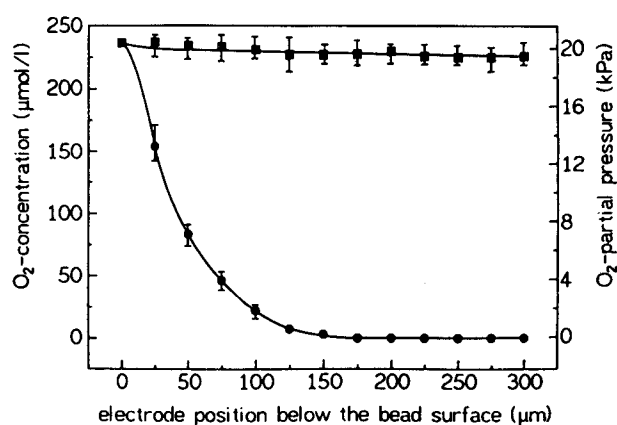


Figure 5. Oxygen concentration in cell-free (■) and cell-loaded (●) alginate beads. Beads loaded with cells of *Enterobacter cloacae* were incubated for 6 h in the fermentation medium. The cell concentration was  $1.93 \times 10^8$  cells per bead. Bars show the deviation between the maximum and minimum data.

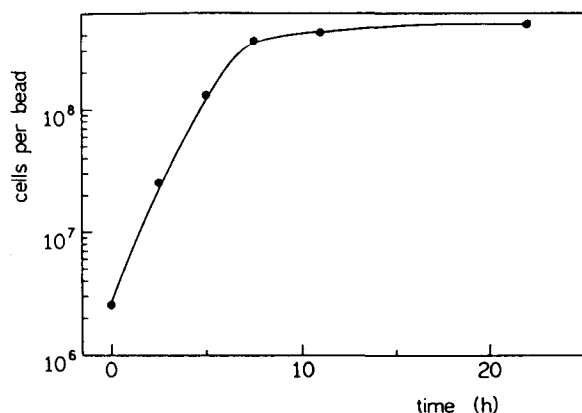


Figure 6. Growth of *Enterobacter cloacae* in Ca-alginate beads.

#### Oxygen gradients in cell-loaded alginate beads in relation to bacterial growth

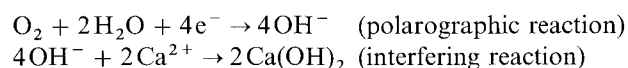
The course of the oxygen concentration gradient inside the cell-loaded alginate beads depended on the bacterial growth in the gel (figs 6, 7A–D). Whereas immediately after immobilization no significant decrease in oxygen concentration was observed (fig. 7A), a concentration gradient had already been formed after 2.5 h of incubation, when the bacterial cells were in the early phase of logarithmic growth (fig. 7B). At the end of this growth-phase (7.5 h of incubation) the gradient showed its most significant shape, with a maximum oxygen penetration depth of about 150  $\mu\text{m}$  (fig. 7C). At this stage nearly 70% of the bead volume is oxygen-free. With further increase of the incubation time the gradient became less steep, as shown in figure 7D for 22 h of incubation.

#### Discussion

Oxygen measurements with  $\text{pO}_2$ -microelectrodes in Ca-alginate are influenced by the effects of mechanical pressure and free Ca-ions, which may interfere with the function of an oxygen microelectrode in such a drastic manner that reasonable measurements become impossible.

The compensation of the pressure effect by periodical step-in and step-out of the microelectrode may be the result of the release of the pressure of the gel on the electrode tip. The occurrence of pressure effects on needle electrodes could also be shown for agar-agar<sup>23</sup> and gelatine<sup>1</sup> gels. The reasons for these effects are not yet known exactly. However, the mechanical pressure is probably able to change the diffusion properties of the membrane and the medium in front of the electrode tip, which affects physico-chemical processes determining the measuring signal.

The disturbance of the electrode function by free Ca-ions may be caused by the membrane being incomplete, so that one main function of this membrane, the protection of the polarographic reaction against disturbing influences from the measuring medium, is cancelled. According to our previous assumptions<sup>3</sup>, free  $\text{Ca}^{2+}$ -ions which reach the Pt-cathode may form  $\text{Ca}(\text{OH})_2$ -precipitates:



The active surface of the cathode will be reduced by this  $\text{Ca}(\text{OH})_2$ -precipitate, and as a consequence the electrode

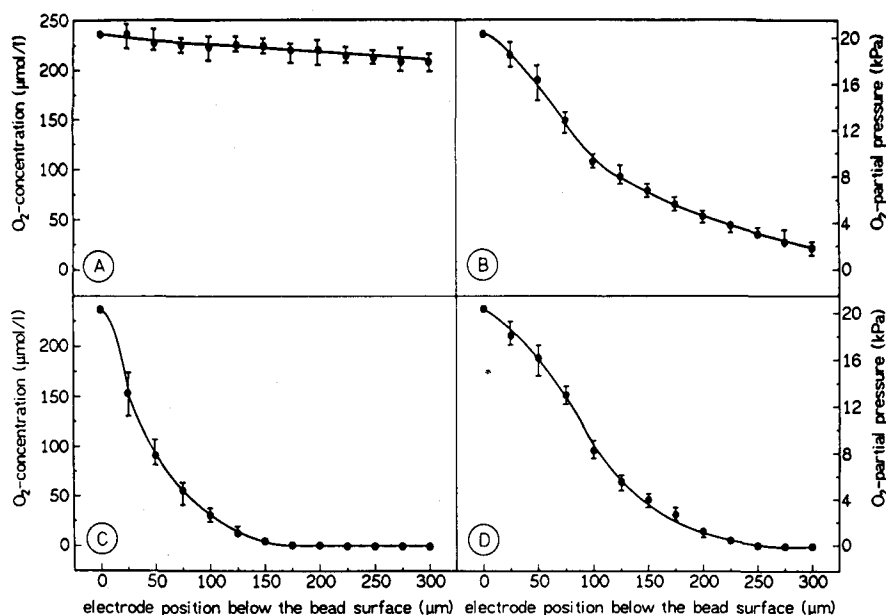


Figure 7. Oxygen gradients in alginate beads loaded with cells of *Enterobacter cloacae* in relation to bacterial growth. A 0 h (immediately after immobilization). B 2.5 h of incubation. C 7.5 h of incubation. D 22 h of

incubation. Bars show the deviation between maximum and minimum data.

signal decreases. Complex-bound  $\text{Ca}^{2+}$ -ions have no interfering influence on the electrode function. This applies to EGTA-bound ions, as well as to alginic acid-bound Ca-ions. An explanation for the observed irregular discharging signal is not yet possible.

Since the oxygen solubility coefficient of the immediate surroundings of the electrode is only approximately known, we have given oxygen concentration as well as the oxygen partial pressure in our figures<sup>16</sup>.

Our experiments showed that by eliminating the effect of pressure, by means of pressure-release, and eliminating the effect of unbound Ca-ions by optimal washing of the beads as well as by complex-binding, oxygen measurements with microelectrodes in Ca-alginate were possible. The oxygen gradients within the cell-loaded gel bead were found to depend on bead-diameter, respiration rate of the entrapped microorganisms,  $\text{O}_2$  mass transfer by diffusion and possibly some convection.

The occurrence of steep oxygen gradients in cell-loaded gel beads elucidates that in our case, under conditions of high respiration rates and diffusion-limited mass transfer, the main volume of the alginate beads used is free of oxygen. This anoxic condition depended on the microbial activity; the oxygen penetration depth was minimal at the end of the logarithmic phase of growth. The attainment of the stationary phase of growth as well as the decrease of the pH in the fermentation medium as a consequence of glucose catabolism by *Enterobacter cloacae* may be the reasons for the increased depth of oxygen penetration after 22 h of incubation. However, even at this stage the greatest part of the bead is free of oxygen. Investigations concerning the effectiveness factor and the oxygen uptake rate of gel-entrapped microbial cells<sup>8, 14</sup> have already led to the assumption that anoxic parts in the center of microbial aggregates may appear. The formation of dense cell layers of aerobic microorganisms only at the periphery of the gel beads and the lack of growth in the central parts of the beads confirm this finding<sup>8, 11, 21</sup>.

The incidence of substantial anoxic parts in microbial immobilisates clearly shows that for aerobic processes with immobilized cells the aggregate diameter has to be very small to ensure a sufficient oxygen supply for all cells. On the other hand, attempts can be made to use the anoxic parts of larger alginate beads for synchronous anaerobic and aerobic processes. In this way the production of ethanol from starch was achieved by coimmobilization of *Aspergillus awamori* and *Zymomonas mobilis*<sup>24</sup>, and of *Aspergillus awamori* and *Saccharomyces cerevisiae*<sup>21</sup>. In a similar way the production of lactic acid from starch was obtained using coimmobilisates of *Aspergillus awamori* and *Streptococcus lactis*<sup>20</sup>. Our own investigations on synchronous reductive and oxidative degradation of xenobiotics by immobilized microorganisms<sup>4</sup> also show the prospective utility of the anoxic parts in microbial aggregates. Further investigations in this field are in progress.

Acknowledgments. We want to thank Prof. Dr R. Kinne (MPI Dortmund) for the facilitation of this cooperative work, Prof. Dr D. W. Lübbers (MPI Dortmund) for his critical remarks on the manuscript and Mrs G. Malinkewitz (MPI Dortmund) for skilful technical assistance.

\* To whom reprint requests should be addressed.

- Baumgärtl, H., Systematic investigations of needle electrode properties in polarographic measurements of local tissue  $\text{pO}_2$  in: Clinical Oxygen Pressure Measurement, p. 17–42. Eds A. M. Ehrly, J. Hauss and R. Huch. Springer, Heidelberg 1987.
- Baumgärtl, H., and Lübbers, D. W., Microcoaxial needle sensor for polarographic measurement of local  $\text{O}_2$  pressure in the cellular range of living tissue. Its construction and properties, in: Polarographic Oxygen Sensors, p. 37–65. Eds E. Gnaiger and H. Forstner. Springer, Heidelberg 1983.
- Baumgärtl, H., and Lübbers, D. W., Die Bedeutung der Membran bei polarographisch arbeitenden  $\text{O}_2$ -Sensoren – insbesondere bei der Mikronadelelektrode – für die absolute  $\text{pO}_2$ -Messung in Flüssigkeiten und Geweben, in: Atemgaswechsel und  $\text{O}_2$ -Versorgung der Organe, p. 155–171. Eds J. Grote and E. Witzleb. Frank Steiner, Stuttgart 1987.
- Beunink, J., and Rehm, H. J., Synchronous anaerobic and aerobic degradation of DDT by an immobilized mixed culture system. Appl. Microbiol. Biotech. 29 (1988) 72–80.
- Bungay, H. R., Whalen, W. J., and Sanders, W. M., Microprobe techniques for determining diffusivities and respiration rates in microbial slime systems, Biotech. Bioeng. 11 (1969) 765–772.
- Chang, H. N., and Moo-Young, M., Estimation of oxygen penetration depth in immobilized cells. Appl. Microbiol. Biotech. 29 (1988) 107–112.
- Chen, Y. S., and Bungay, H. R., Microelectrode studies of oxygen transfer in trickling filter slimes. Biotech. Bioeng. 23 (1981) 781–792.
- Chen, K.-Ch., and Huang, Ch.-T., Effects of the growth of *Trichosporon cutaneum* in calcium alginate gel beads upon bead structure and oxygen transfer characteristics. Enzyme Microb. Technol. 10 (1988) 284–292.
- Chen, T. L., and Humphrey, A. E., Estimation of critical particle diameters for optimal respiration of gel entrapped and/or pelletized microbial cells. Biotech. Lett. 10 (1988) 699–702.
- Eikmeier, H., and Rehm, H. J., Stability of calcium-alginate during citric acid production of immobilized *Aspergillus niger*. Appl. Microbiol. Biotech. 26 (1987) 105–111.
- Eikmeier, H., Westmeier, F., and Rehm, H. J., Morphological development of *Aspergillus niger* immobilized in Ca-alginate and  $\kappa$ -carrageenan. Appl. Microbiol. Biotech. 12 (1984) 53–57.
- Enfors, S. O., and Mattiasson, B., Oxygenation of processes involving immobilized cells, in: Immobilized cells and Organelles, vol. II, p. 41–60. Ed. B. Mattiasson. CRC-Press, Boca Raton 1983.
- Gosman, B., and Rehm, H. J., Oxygen uptake of microorganisms entrapped in Ca-alginate. Appl. Microbiol. Biotech. 23 (1986) 163–167.
- Gosmann, B., and Rehm, H. J., Influence of growth behaviour and physiology of alginate entrapped microorganism on the oxygen consumption. Appl. Microbiol. Biotech. 29 (1988) 554–559.
- Huang, M. Y., and Bungay, H. R., Microprobe measurements of oxygen concentrations in mycelial pellets. Biotech. Bioeng. 15 (1973) 1193–1197.
- Hutten, H., Meiners, K., and Zander, R., Ein polarographisches Verfahren zur Bestimmung von Sauerstoff-Löslichkeitskoeffizienten in wäßrigen Elektrolytlösungen. Biomed. Technol. 27 (1982) 7–13.
- Karube, I., Kuriyama, S., Matsunaga, T., and Suzuki, S., Methane production from wastewaters by immobilized methanogenic bacteria. Biotech. Bioeng. 22 (1980) 847–857.
- Karube, I., Matsunaga, T., Otomine, Y., and Suzuki, S., Nitrogen fixation by immobilized *Azotobacter chroococcum*. Enzyme Microbiol. Technol. 3 (1981) 309–312.
- Kokufuta, E., Shimohashi, M., and Nakamura, I., Simultaneously occurring nitrification and denitrification under oxygen gradient by polyelectrolyte complex-coimmobilized *Nitrosomonas europaea* and *Paracoccus denitrificans*. Biotech. Bioeng. 31 (1988) 382–384.
- Kurosawa, H., Ishikawa, H., and Tanaka, H., L-Lactic acid production from starch by coimmobilized mixed culture system of *Aspergillus awamori* and *Streptococcus lactis*. Biotech. Bioeng. 31 (1988) 183–187.
- Kurosawa, H., Nomura, N., and Tanaka, H., Ethanol production from starch by a coimmobilized mixed culture system of *Aspergillus*

- awamori* and *Saccharomyces cerevisiae*. Biotech. Bioeng. 33 (1989) 716–723.
- 22 Pfennig, N., and Lippert, K. D., Über das Vitamin B<sub>12</sub>-Bedürfnis phototropher Schwefelbakterien. Archs Microbiol. 55 (1966) 245–256.
- 23 Schuchhardt, S., and Lösse, B., Methodological problems when measuring with pO<sub>2</sub>-needle electrodes in semisolid media. in: Oxygen Supply, p. 108–109. Eds M. Kessler, D. F. Bruley, L. C. Clark, D. W. Lübbers, I. A. Silver and J. Strauss. Urban & Schwarzenberg, München 1973.
- 24 Tanaka, H., Kurosawa, H., and Murakami, H., Ethanol production from starch by a coimmobilized mixed culture system of *Aspergillus awamori* and *Zymomonas mobilis*. Biotech. Bioeng. 28 (1986) 1761–1768.
- 25 Wittler, R., Baumgärtl, H., Lübbers, D. W., and Schügerl, K., Investigations of oxygen transfer into *Penicillium chrysogenum* pellets by microprobe measurements. Biotech. Bioeng. 28 (1986) 1024–1036.

0014-4754/89/11-12/1041-07\$1.50 + 0.20/0

© Birkhäuser Verlag Basel, 1989

## Physical methods for characterization of microbial cell surfaces

C. Krekeler, H. Ziehr and J. Klein

GBF, Gesellschaft für Biotechnologische Forschung, Mascheroder Weg 1, D-3300 Braunschweig (Federal Republic of Germany)

**Summary.** There are different concepts for explaining the adsorption of microorganisms to solid surfaces: the DLVO theory and the surface free energy. Basic aspects of both theories are discussed. Established methods for determining the surface properties of microbial cells are reviewed: Electrophoretic mobility, colloid titration, electrostatic interaction chromatography, bacterial adherence to hydrocarbons, partitioning in an aqueous two-phase system, hydrophobic interaction chromatography, contact angle measurement and X-ray photoelectron spectroscopy. They are discussed and classified according to their potential for the correlation of cell surface characteristics and adsorption behavior.

**Key words.** Cell surface characterization; surface charge; hydrophobicity; chemical analysis; adsorption.

### Introduction

Up to now no uniform theory has been developed to explain the fundamental mechanisms of cell adsorption phenomena. Both physical and chemical theories have been proposed<sup>23</sup>. One can distinguish between reversible adsorption, where the microorganisms still exhibit Brownian motion and can be removed from the surface by shearing forces, and irreversible adsorption where the microorganisms are firmly attached to the surface by extracellular polymer fibrils (polymer bridging) or by specific cell adhesion molecules (adhesines), which are supposed to be responsible for selective interactions between microorganisms and plants or animal or human tissues<sup>49</sup>.

The present paper is focussed on the influence of physical interactions on adsorption. Such interactions can be classified as long-range (distances > 150 nm), short-range (distances < 150 nm) and very short-range forces (distances < 50 nm)<sup>87</sup>. The DLVO theory, developed by Derjaguin, Landau, Verwey and Overbeek, is applicable in general to explain long-range interactions<sup>73</sup>. According to this theory the total interaction energy of two particles ( $V_T$ ) is calculated by the sum of the London-van der Waals attractive ( $V_A$ ) and the electrostatic-like-charge repulsive energy ( $V_R$ ). The repulsive energy depends on the thickness of the electrical double layer, which is inversely correlated to the ionic strength of the suspending liquid<sup>49</sup>; on the surface potential; on the distance be-

tween the interacting particles, and on the dielectric constant of the liquid phase<sup>73, 87</sup>. If the electrical double layer is small, attractive interactions even between surfaces of the same charge are possible. Figure 1 shows the correlation of the interaction energy ( $V_T$ ) and the distance ( $h$ ) between like-charge particles; attraction occurs at the primary and at the secondary minimum ( $h = 5–10$  nm). Though for biological systems the exact determination of the terms  $V_A$  and  $V_R$  is difficult, the DLVO theory may be useful for the interpretation of adsorption phenomena<sup>73</sup>.

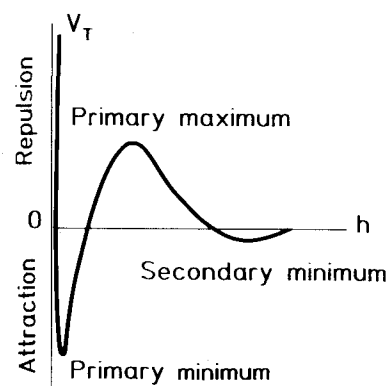


Figure 1. Correlation of the total interaction energy ( $V_T$ ) between two particles of the same charge and the separation distance ( $h$ ). (Barclay et al.<sup>10</sup> and Rutter<sup>73</sup>, modified).